Molecular & Cellular Toxicology (2021) 17:201–212
https://doi.org/10.1007/s13273-021-00126-9

ORIGINAL ARTICLE

KIF11 inhibition decreases cytopathogenesis and replication of influenza A virus

Dong-In Kim[1] · Ji-Hun Kang[1] · Eui-Ho Kim[2] · Young-Jin Seo[1]

Accepted: 10 February 2021 / Published online: 26 February 2021

Abstract

Background Seasonal flu is an infectious disease of the respiratory tract caused by influenza viruses. The development of anti-influenza drugs has significantly reduced the threat from the influenza virus; however, frequent mutations of this negative RNA virus result in antiviral-resistant strains, and constantly intimidate the human race. Thus, identifying novel therapeutic targets for the prevention and treatment of influenza virus infections is critical.

Objective We aimed to determine whether the kinesin superfamily protein 11 (KIF11) inhibitors, monastrol and K858, inhibit viral cytopathogenesis and influenza A virus (IAV) replication.

Result When MDCK or HEK293 cells were treated with monastrol and K858 that did not induce significant cytotoxicity, IAV-induced cytopathic effect was attenuated significantly. Furthermore, these inhibitors effectively suppressed the production of viral RNA, proteins, and infectious viral particles.

Conclusion Inhibition of KIF11 activity effectively attenuates virus-mediated cytopathic effect and suppresses viral replication. Hence, KIF11 is a potential therapeutic target against the influenza virus.

Keywords KIF11 · Influenza A virus · Viral cytopathogenesis · Anti-viral drug

Introduction

The influenza virus is one of the most common causes of acute respiratory infections that result in a significant health burden. Influenza virus infections induce significant cell death within the upper and lower respiratory tract and lung parenchyma, which causes respiratory symptoms such as fever, chills, fatigue, and coughs, and pneumonia in some severe cases particularly in the elderly (Atkin-Smith et al. 2018). As a lytic virus, the influenza virus destroys host cells through both intrinsic and extrinsic apoptotic pathways to produce progeny viruses (Galluzzi et al. 2018). Multiple resistant strains have emerged against the currently available anti-influenza virus drugs such as oseltamivir and amantadine (Cheng et al. 2010; Dharan et al. 2009; Heo et al. 2018; Marjuki et al. 2015a, b), raising concerns of a pandemic. Thus, identifying novel host factors associated with influenza virus replication and cytotoxicity is important.

Kinesins are ATP-dependent motor proteins that transport intracellular molecules along microtubules. To date, 45 kinesin family protein (KIF) genes, grouped into 14 families (kinesin-1–kinesin-14), have been identified in humans and mice (Miki et al. 2001). Given the critical role of the intracellular transport system in viral assembly and release (Bedi and Ono 2019; Cudmore et al. 1997; Radtke et al. 2006; Smith and Helenius 2004; Sodeik 2000; Wolfstein et al. 2004), several studies have been conducted on the role of KIFs in the viral life cycle. Studies have shown direct involvement of KIF13A and KIF18A in influenza A virus replication and cytopathogenesis (Cho et al. 2020;

Dong-In Kim and Ji-Hun Kang contributed equally to this study.

✉ Young-Jin Seo
yjseo@cau.ac.kr

Dong-In Kim
kdi0908@cau.ac.kr

Ji-Hun Kang
kss1587@cau.ac.kr

Eui-Ho Kim
euiho.kim@ip-korea.org

[1] Department of Life Science, College of Natural Sciences, Chung-Ang University, 84 Heukseok-ro, Dongjak-gu, Seoul 06974, Korea

[2] Viral Immunology Laboratory, Institut Pasteur Korea, Seoul, Korea

Ramos-Nascimento et al. 2017). Furthermore, KIF3A, KIF4, and KIF5 have been shown to play important roles in viral life cycle regulation, including in the HIV, herpes simplex, and Lassa viruses.

KIF11 (also known as kinesin-5 or Eg5) is a kinesin superfamily protein known to regulate mitotic spindle formation (Valentine et al. 2006; Waitzman and Rice 2014) and microtubule extension (Chen and Hancock 2015). Because several KIFs are associated with the viral life cycle, we investigated the role of KIF11 in influenza A virus (IAV) replication and cytopathogenesis to determine whether KIF11 could be a therapeutic target against IAV.

Materials and methods

Cells and virus

Madin–Darby Canine kidney (MDCK) cells were cultured in a minimum essential medium (MEM, GenDEPOT, TX), and human embryonic kidney 293 (HEK) were cultured in a Dulbecco-modified Eagle medium (DMEM, GenDEPOT, TX). Cell culture media were supplemented with 10% fetal bovine serum (FBS, GenDEPOT, TX) and 1% penicillin/streptomycin (Wellgene, Gyeongsan, Korea). Influenza A/California/2007 (H1N1) viruses were provided by Dr. Sang-Myeong Lee (Chungbuk National University, Korea). IAV amplification and titration were conducted with MDCK cells. For the infection, MDCK or HEK 293 cells were incubated with IAV for 1 h in a medium containing 0.3% bovine serum albumin (BSA) and TPCK-trypsin (2 μg/mL).

KIF11 inhibitors and antibodies

Monastrol and K858 were purchased from Sigma-Aldrich (Saint Louis, MO). Antibodies used to detect influenza virus matrix protein (M1) and nucleoprotein (NP) were purchased from Abcam (Cambridge, UK), and the anti-influenza virus NS1 antibody was purchased from Santa Cruz Biotechnology (Dallas, TX).

Analysis of cytopathic effect

The MDCK and HEK 293 cells were seeded at 1×10^5 cells per well in 24-well plates. After 24 h, cells were infected with IAV in the presence or absence of monastrol and K858 at concentrations of 10 and 20 μM, respectively, and incubated for 24 h. Subsequently, the medium was removed, cells were washed thrice with PBS, and fixed with 4% formaldehyde (SAMCHUN, Seoul, Korea) for 10 min. The cells were then stained with 1% crystal violet (Sigma-Aldrich, Saint Louis, MO) dye solution to visualize IAV-induced cytopathic effect (CPE) cytopathy.

Trypan blue exclusion assay

To determine cell viability, 100 μL cell suspension was mixed with an equal volume of trypan blue dye solution (0.4%). After incubation for 1 min, cells were analyzed under a light microscope. Trypan blue-unstained cells were considered viable, and the stained cells were considered dead.

Flow cytometric analysis

To evaluate apoptosis, the annexin V apoptosis detection kit (BioLegend, San Diego, CA) was used according to the manufacturer's instructions. We also performed 7-amino actinomycin D (7-AAD) staining to detect early apoptotic cells. To analyze intracellular influenza viral protein expression, cells were permeabilized using the Foxp3/transcription factor staining kit (Tonbo Biosciences, San Diego, CA), followed by incubation with anti-influenza viral M1 or NP antibodies (Abcam, Cambridge, UK) for 2 h. Cells were then incubated with Alexa Fluor 488-conjugated secondary antibodies for 1 h (Thermo Scientific, Waltham, MA). Data were collected using an Attune NxT acoustic focusing cytometer (Thermo Scientific, Waltham, MA) and analyzed using FlowJo software (BD Bioscience, NJ, USA).

Western blot analysis

Western blot analysis was performed as described previously (Cho et al. 2020). Briefly, cell lysates (10 μg protein) were loaded onto SDS-PAGE gels and then transferred onto nitrocellulose membranes. After incubation with primary and secondary antibodies, target protein expression was detected using the SuperSignal West Pico Plus chemiluminescent substrate (Thermo Scientific, Waltham, MA).

Plaque assay

For IAV titration, MDCK cells were incubated with a cell supernatant containing IAV for 1 h. Cells were then overlaid

with 1% agarose diluted in MEM containing 0.3% BSA. After 3 days, the cells were fixed with 3.5% formaldehyde and stained with 1% crystal violet (Sigma-Aldrich, MO, USA) dye solution for plaque visualization.

Real-time quantitative PCR

After total RNA extraction using the RNAiso Plus reagent (Takara, Shiga, Japan), cDNA was synthesized using the RevertraAce qPCR RT kit (Toyobo, Osaka, Japan). Real-time quantitative PCR for viral RNAs (M1, NP) was performed using the CFX Connect real-time system (Bio-Rad, Hercules, CA) with the following primers: GAPDH forward, 5′-TGGACCTGACCTGCCGTCTA-3′, reverse 3′-CCCTGTTGCTGTAGCCAAATTC-3′; M1 forward, 5′-AAGACCAATCCTGTCACCTCTG-3′, reverse 5′-CAAAACGTCTACGCTGCAGTCC-3′; NP forward 5′-CCAGATCAGTGTGCAGCCTA-3′, reverse, 5′-CTTCTGGCTTTGCACTTTCC-3′. The threshold cycle number for each sample was determined in quintuplicates and normalized with GAPDH.

Immunocytochemistry

HEK 293 cells with or without IAV infection were plated on a chamber slide (Millipore, Burlington, MA). After incubation with the indicated condition, cells were fixed with 4% formaldehyde and then permeabilized with 0.5% Triton X-100. The cells were incubated with anti-influenza virus NP antibodies (1 μg/mL; Abcam, Cambridge, UK) and then stained with Alexa Fluor 488-conjugated secondary antibodies (Thermo Scientific, Waltham, MA). Cells were mounted on the slides with the Fluoroshield mounting medium containing DAPI (Thermofisher, MA, USA). Images were collected using an LSM710 confocal microscope (Carl Zeiss, Oberkochen, Germany) and analyzed using LSM Image Browser (Carl Zeiss, Oberkochen, Germany).

Statistical analysis

All experiments were performed at least thrice with consistent results. Error bars represented the standard error of mean (SEM), and *P* values were analyzed using the Student's *t* test with the Prism 5 software (GraphPad software, La Jolla, CA).

Results

Optimal concentration of KIF11 inhibitors

To inhibit KIF11 activity, the highly specific small-molecule inhibitors monastrol and K858 were used. We first determined the optimal concentration of each inhibitor that did not cause significant cytotoxicity. First, the MDCK and HEK293 cells were treated with varying concentrations of monastrol and K858. At 24 h after treatment, cell viability was evaluated using the trypan blue exclusion assay. Treatment with 100 or 200 μM of monastrol significantly reduced MDCK (Fig. 1a) and HEK293 (Fig. 1b) cell viability. Similarly, 100 or 200 μM of K858 significantly reduced the viability of MDCK (Fig. 1c) and HEK 293 (Fig. 1d) cells. In addition, we assessed the morphological changes in MDCK and HEK 293 cells after treatment with the inhibitors. Treatment with 50, 100, or 200 μM of monastrol (Fig. 1e, f) or K858 (Fig. 1g, h) induced notable morphologic changes and detachment of both HEK293 (Fig. 1f, g) and MDCK cells (Fig. 1e, g) in a dose-dependent manner; lower doses (10 or 20 μM) of the inhibitors did not induce notable changes. Because dead cells lose the ability to remain attached to the plate surface and undergo morphologic changes such as cell shrinking, these results indicate that high concentrations (> 50 μM) of monastrol and K858 exhibit cytotoxicity.

Monastrol and K858 induce apoptosis-mediated cell death at high concentrations

Although we observed cell death and changes in cell morphology (Fig. 1), these results do not demonstrate whether high concentrations of KIF11 inhibitors induce apoptotic cell death. Therefore, we attempted to assess whether KIF11 inhibitor-induced cytotoxicity is apoptosis mediated. Cells were treated with varying concentrations of monastrol or K858 for 24 h and probed with annexin V and 7-AAD staining to quantify apoptosis (Fig. 2a, b). High concentrations (100 and 200 μM) of both monastrol and K858 dramatically increased early apoptotic (annexin V^+/7-AAD^-) and late apoptotic (annexin V^+/7-AAD^+) populations. These results indicate that higher concentrations of monastrol and K858 induced apoptosis-mediated cytotoxicity. Therefore, we used

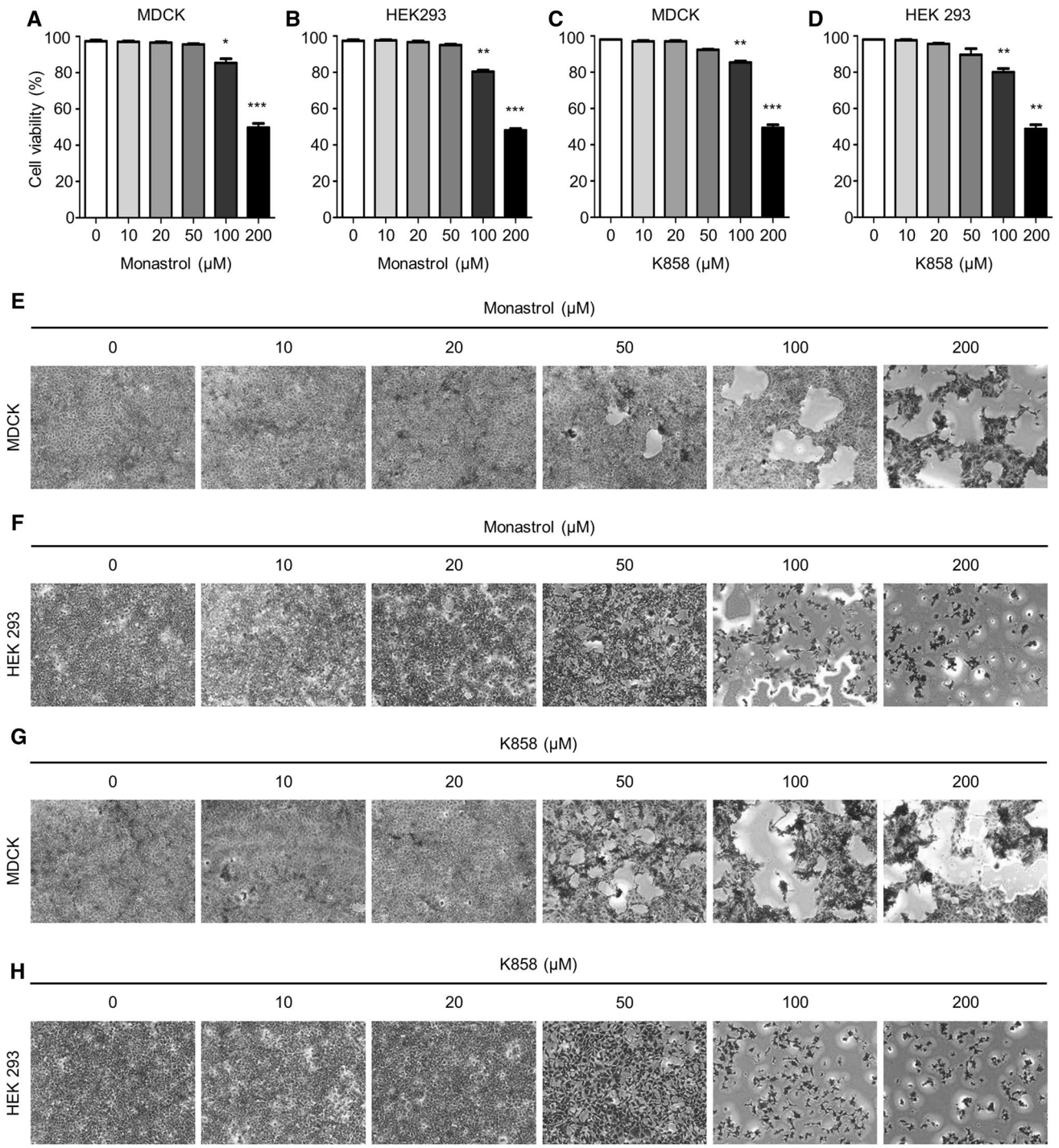

Fig. 1 High concentrations of monastrol and K858 exhibit cytotoxicity. MDCK (**a**, **c**) or HEK293 cells (**b**, **d**) were cultured for 24 h with or without monastrol (10, 20, 50, 100, or 200 μM) (**a**, **b**) and K858 (10, 20, 50, 100, or 200 μM) (**c**, **d**). Cell viability was measured using a trypan blue exclusion assay. *N.S.* not significant; $^{**}P < 0.01$; $^{***}P < 0.001$. MDCK (**e**, **g**) or HEK293 cells (**f**, **h**) were cultured for 24 h with or without monastrol (10, 20, 50, 100, or 200 μM) (**e**, **f**) and K858 (10, 20, 50, 100, or 200 μM) (**g**, **h**) and then stained with 1% crystal violet solution

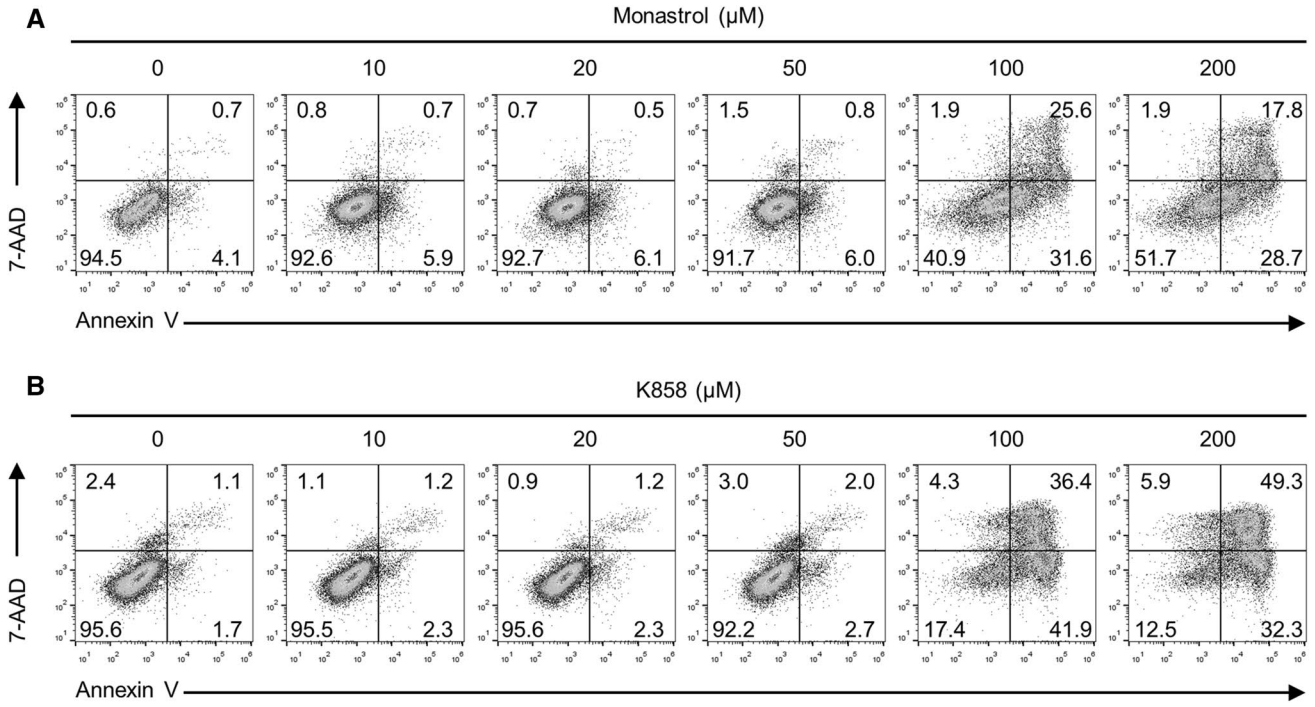

Fig. 2 Monastrol or K858 effect apoptosis-mediated cell death. MDCK cells untreated or treated with monastrol (10, 20, 50, 100, or 200 μM) (**a**) or K858 (10, 20, 50, 100, or 200 μM) (**b**) were compared. At 24 h after treatment, cells were stained with PE-conjugated annexin V and 7-AAD and assayed using flow cytometry. Percentages of annexin V ±, 7-AAD ± populations are shown

lower concentrations of these inhibitors (10 and 20 μM) for subsequent experiments to avoid significant cell death.

KIF11 inhibition prevents IAV-induced cytopathic effect

IAV is a lytic virus and hence IAV infection causes CPE in infected cells. Therefore, we examined whether KIF11 inhibition also affects IAV infection-triggered cytotoxicity. As expected, H1N1 influenza virus infection caused significant CPE in both MDCK and HEK 293 cells when measured using crystal violet staining (Fig. 3a, c, e, g) and trypan blue exclusion assay (Fig. 3b, d, f, h). Of interest, IAV-induced CPE in MDCK (Fig. 3a, b, e, f) and HEK 293 cells (Fig. 3c, d, g, h) was significantly attenuated by treatment with 10 or 20 μM of monastrol and K858. Thus, these results indicate that KIF11 inhibition protects host cells from IAV infection-induced CPE.

KIF11 inhibition attenuates IAV replication

Because KIFs such as KIF13 and KIF18A are associated with viral replication (Cho et al. 2020; Ramos-Nascimento et al. 2017), we hypothesized that the inhibition of KIF11

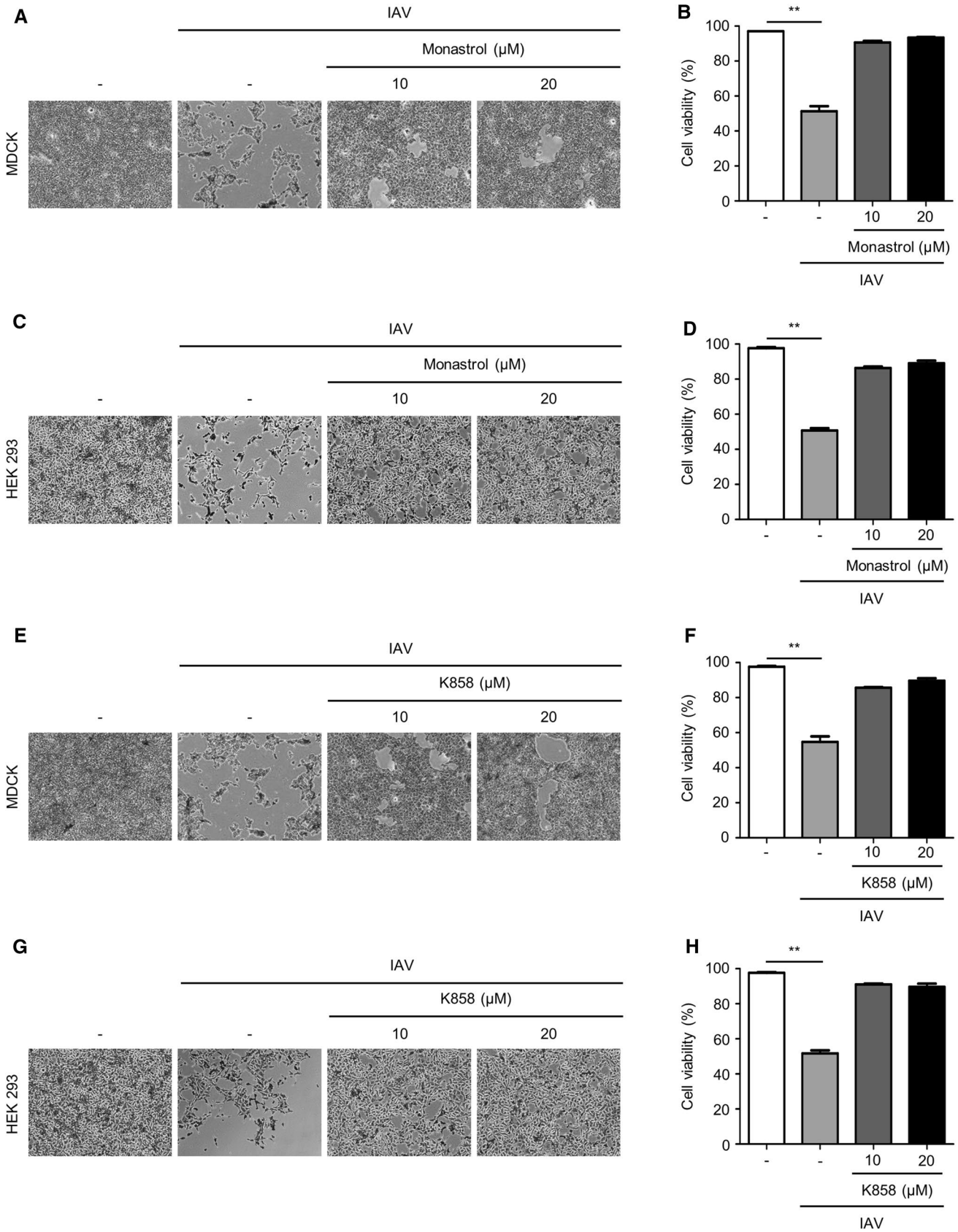
A
IAV
Monastrol (μM)
-
-
10
20
MDCK
B
**
Cell viability (%)
100
80
60
40
20
0
-
-
10
20
Monastrol (μM)
IAV
C
IAV
Monastrol (μM)
-
-
10
20
HEK 293
D
**
Cell viability (%)
100
80
60
40
20
0
-
-
10
20
Monastrol (μM)
IAV
E
IAV
K858 (μM)
-
-
10
20
MDCK
F
**
Cell viability (%)
100
80
60
40
20
0
-
-
10
20
K858 (μM)
IAV
G
IAV
K858 (μM)
-
-
10
20
HEK 293
H
**
Cell viability (%)
100
80
60
40
20
0
-
-
10
20
K858 (μM)
IAV

◂ **Fig. 3** Monastrol or K858 treatment protects host cells from IAV-induced cytopathy. MDCK (**a**, **b**) or HEK293 cells (**c**, **d**) with (0.1 MOI) or without IAV infection with or without monastrol treatment (10 or 20 μM) for 24 h were compared. MDCK (**e**, **f**) or HEK293 cells (**g**, **h**) with (0.1 MOI) or without IAV infection with or without K858 treatment (10 or 20 μM) for 24 h were compared. Cell morphology changes were analyzed following staining with 1% crystal violet solution (**a**, **c**, **e**, **g**) and cell viability was assessed using a trypan blue exclusion assay (**b**, **d**, **f**, **h**)

will suppress IAV replication. We first compared the amount of viral RNA in IAV-infected cells in the presence or absence of KIF11 inhibitors. Real-time quantitative PCR was used to measure M1 and NP expression levels. A significant dose-dependent decrease in M1 and NP expression levels was observed when cells were treated with monastrol (Fig. 4a, b) and K858 (Fig. 4c, d). Similarly, the Western blot analysis revealed a significant decrease in M1 and NS1 expression levels with monastrol (Fig. 4e, f) and K858 (Fig. 4g, h) treatment in both MDCK (Fig. 4e, g) and HEK 293 cells (Fig. 4f, h). Finally, we determined whether the production of infectious viral particles was decreased by KIF11 inhibition. A significant decrease in the production of viral particles was seen with monastrol (Fig. 4i) and K858 (Fig. 4j) treatment. Overall, these results confirm that KIF11 inhibition hinders IAV replication in host cells.

KIF11 inhibition decreases the proportion of IAV-infected cells

We further examined whether monastrol and K858 treatments affected the proportion of IAV-infected cells. MDCK cells were infected with IAV and treated with monastrol (Fig. 5a, b) and K858 (Fig. 5c, d). Flow cytometric analysis of viral M1 or NP expression was performed. The proportion of MDCK cells expressing viral M1 (Fig. 5a, c) or NP (Fig. 5b, d) significantly decreased with KIF11 inhibitor in a dose-dependent manner. Consistent with this result, the number of viral NP-containing cells declined significantly with monastrol (Fig. 6a) and K858 (Fig. 6b) treatments, as assessed using immunofluorescence. Therefore, KIF11 inhibition diminishes the number of IAV-infected cells.

Discussion

Our results demonstrated the critical protective roles of KIF11 in host cells against IAV infection. KIF11 inhibition with monastrol and K858 resulted in a significant reduction in viral replication and production of infectious viral particles, protecting the host cells from IAV-induced CPE. Several possible mechanisms explain our observations. First,

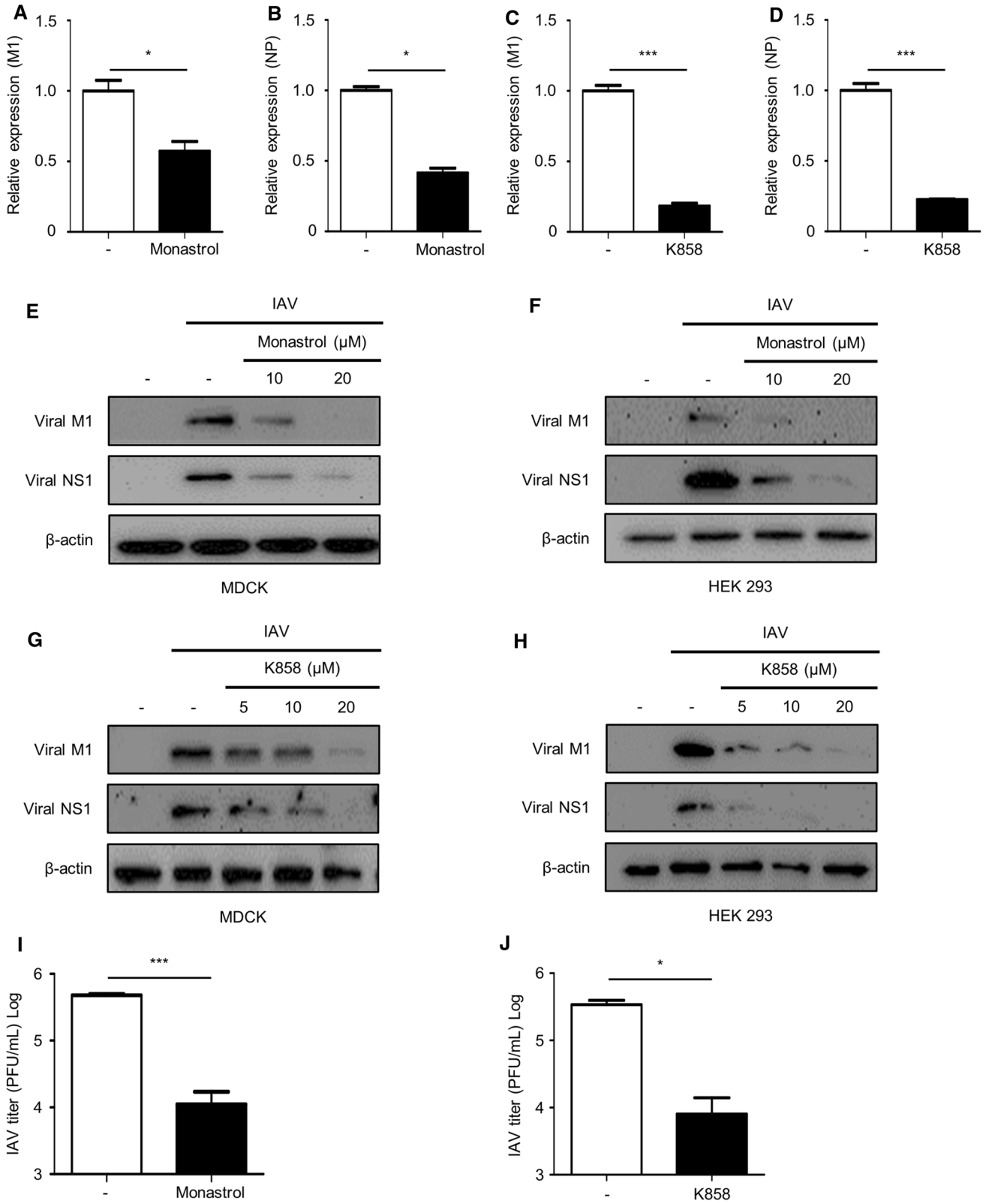
A
Relative expression (M1)
1.5
1.0
0.5
0
*
-
Monastrol
B
Relative expression (NP)
1.5
1.0
0.5
0
*
-
Monastrol
C
Relative expression (M1)
1.5
1.0
0.5
0
***
-
K858
D
Relative expression (NP)
1.5
1.0
0.5
0
***
-
K858
E
IAV
Monastrol (μM)
- - 10 20
Viral M1
Viral NS1
β-actin
MDCK
F
IAV
Monastrol (μM)
- - 10 20
Viral M1
Viral NS1
β-actin
HEK 293
G
IAV
K858 (μM)
- - 5 10 20
Viral M1
Viral NS1
β-actin
MDCK
H
IAV
K858 (μM)
- - 5 10 20
Viral M1
Viral NS1
β-actin
HEK 293
I
IAV titer (PFU/mL) Log
6
5
4
3
***
-
Monastrol
J
IAV titer (PFU/mL) Log
6
5
4
3
*
-
K858

◂**Fig. 4** Monastrol and K858 inhibit IAV replication. HEK293 cells were infected with IAV at 0.1 MOI with or without monastrol (**a**, **b**) or K858 (**c**, **d**) treatment for 12 h. The expression levels of viral M1 (**a**, **c**) and NP (**b**, **d**) were determined using real-time quantitative PCR. MDCK (**e**, **g**) and HEK293 (**f**, **h**) cells were infected with IAV at 0.1 MOI with or without monastrol (**e**, **f**) or K858 treatment (**g**, **h**) for 18 h were compared. The expression of viral M1, NS1, and β-actin was analyzed using Western blotting. MDCK cells with or without IAV infection at 0.01 MOI and untreated with or without 20 μM monastrol (**i**) or 10 μM K858 (**j**) treatment for 24 h were compared. The viral titer was analyzed using a plaque assay. $*P < 0.05$; $***P < 0.001$

kinesins could affect the movement of viral components. Because kinesins are motor proteins transporting intracellular vesicles and molecules, KIF11 inhibition could attenuate the trafficking of viral components essential to viral replication. Second, KIF11 inhibition possibly interferes with the activation of host signaling pathways required for viral replication. Kinesin motors contribute to the trafficking of scaffolds for signaling pathways (Schnapp 2003); KIF11 inhibition likely hinders the activation of signaling pathways associated with viral replication. Third, KIF11 may play a role in the nuclear export of viral ribonucleoprotein (vRNP) complexes. A previous study reported that KIF18A is a regulatory factor for the nuclear export of vRNP complexes (Cho et al. 2020). Thus, it is possible that KIF11 inhibition interferes with the nuclear export of vRNP complexes, resulting in attenuated IAV replication.

Frequent mutations in the RNA genome of influenza viruses has limited the development of anti-viral therapeutics. For instance, the currently available anti-influenza virus drugs such as oseltamivir only have limited efficacy owing to the emergence of drug-resistant variants. Targeting host factors that are critical to viral replication could be an alternative strategy to avoid antiviral resistance. Targeting multiple such host factors in addition to viral factors would likely enhance the efficacy of antiviral therapeutics to a broad spectrum of viral strains. Our study shows that the host factor KIF11 could be a novel and attractive therapeutic target against IAV infection.

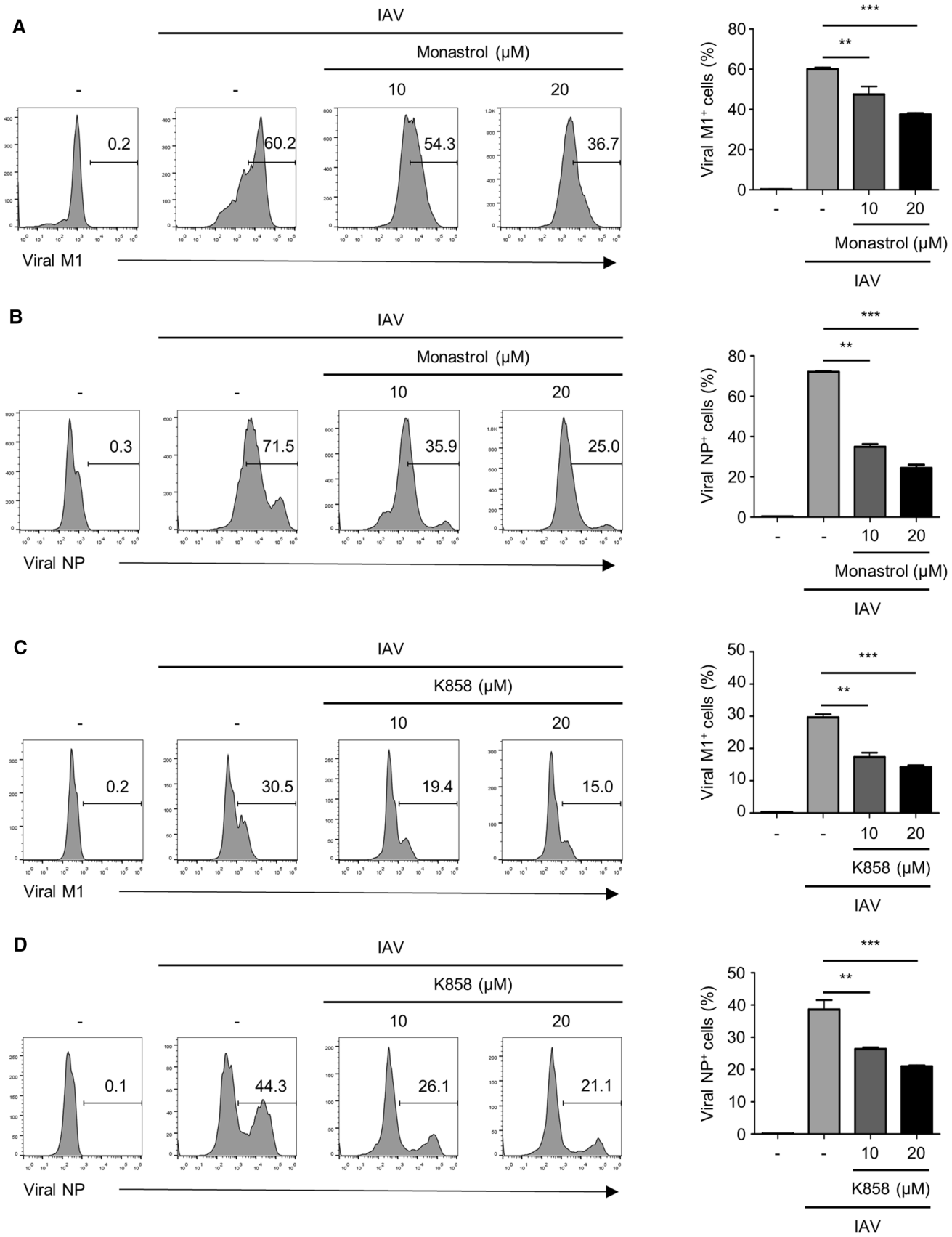
A
IAV
Monastrol (μM)
-
-
10
20
0.2
60.2
54.3
36.7
Viral M1
Viral M1+ cells (%)
***
**
B
IAV
Monastrol (μM)
0.3
71.5
35.9
25.0
Viral NP
Viral NP+ cells (%)
C
IAV
K858 (μM)
0.2
30.5
19.4
15.0
Viral M1
Viral M1+ cells (%)
D
IAV
K858 (μM)
0.1
44.3
26.1
21.1
Viral NP
Viral NP+ cells (%)

◂**Fig. 5** Monastrol and K858 treatment decrease the proportion of IAV-infected cells. MDCK cells with or without infection with IAV at an MOI of 1 (M1) or 0.1 (NP) with or without monastrol (**a**, **b**) or K858 (**c**, **d**) treatment were compared. At 12 or 24 h after infection (hpi), cells were harvested and assayed for viral M1 (**a**, **c**, 12 hpi) or NP (**b**, **d**, 24 hpi) expression using a flow cytometer. Percentages of viral protein-expressing cells ± standard errors of the mean are shown. $^{**}P < 0.01$; $^{***}P < 0.001$

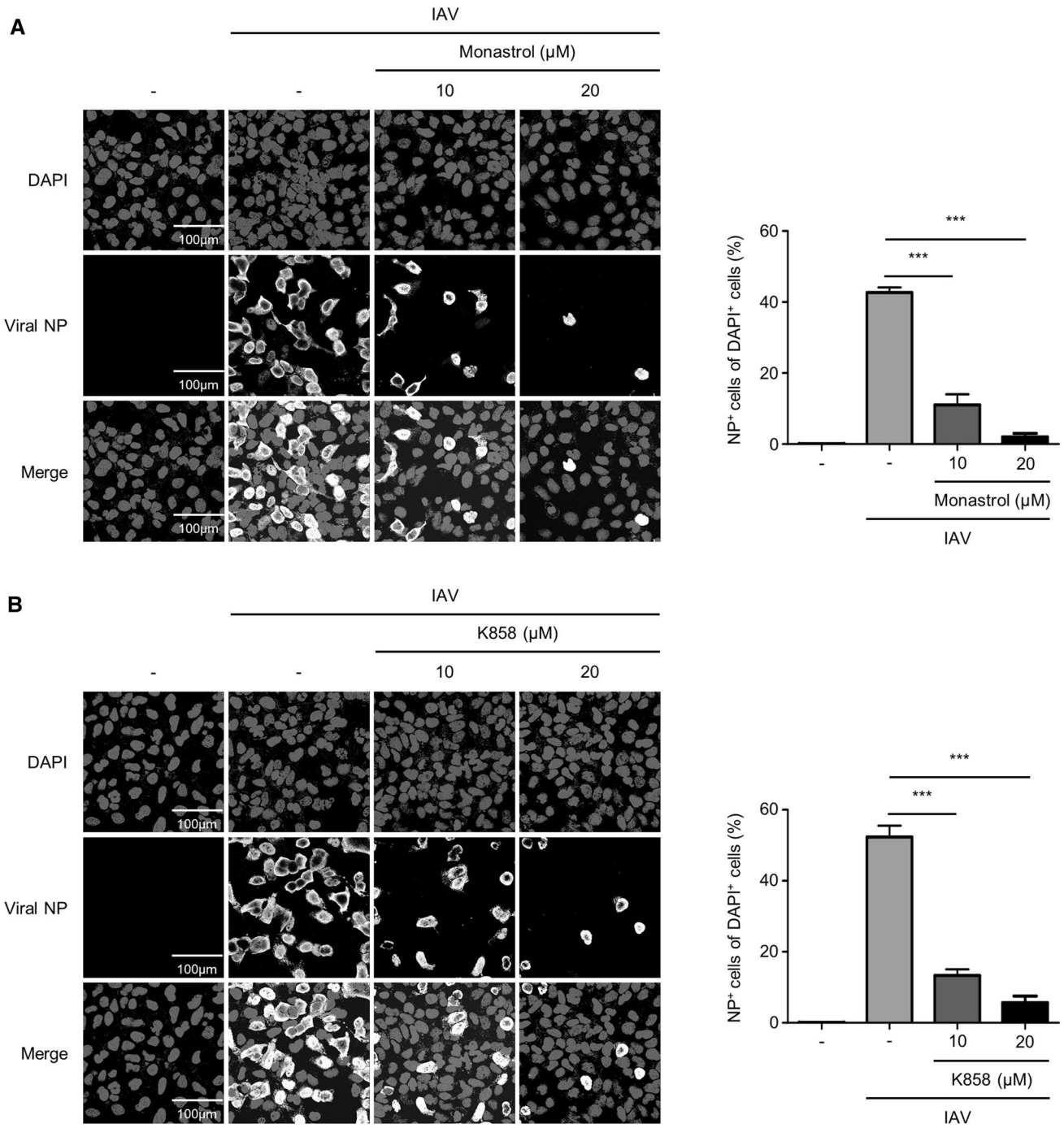

Fig. 6 KIF11 inhibition reduces the number of viral protein-expressing cells. HEK293 cells with or without IAV infection at 3 MOI with or without monastrol (**a**) or K858 (**b**) treatment for 12 h were compared. Viral NP-expressing cells (white) were quantified using a confocal laser scanning microscope. Nuclei were stained with DAPI (gray). The percentages of NP + cells ± standard errors of mean are shown. $^{***}P < 0.001$

Acknowledgements This research was supported by the National Research Foundation of Korea (NRF) Grant funded by the Korea government (MSIT) (no. 2017M3A9G6068245, NRF-2018R1A5A1025077, and 2020R1F1A1069924).

Author contributions Conceptualization, Y-JS; Methodology and investigation, J-HK and D-IK; Data analysis, J-HK, D-IK, E-HK; Statistical analysis, J-HK and D-IK; Writing—original draft, J-HK, D-IK, E-HK, and Y-JS.

Compliance with ethical standards

Conflict of interest The authors declare no conflicts of interest.

Ethical approval The article does not contain any studies on humans or animals.

References

Atkin-Smith GK, Duan M, Chen W, Poon IKH (2018) The induction and consequences of Influenza A virus-induced cell death. Cell Death Dis 9:1002

Bedi S, Ono A (2019) Friend or foe: the role of the cytoskeleton in influenza A virus assembly. Viruses 11:46

Chen Y, Hancock WO (2015) Kinesin-5 is a microtubule polymerase. Nat Commun 6:8160

Cheng PK, To AP, Leung TW, Leung PC, Lee CW, Lim WW (2010) Oseltamivir- and amantadine-resistant influenza virus A (H1N1). Emerg Infect Dis 16:155–156

Cho YB, Hong S, Kang KW, Kang JH, Lee SM, Seo YJ (2020) Selective and ATP-competitive kinesin KIF18A inhibitor suppresses the replication of influenza A virus. J Cell Mol Med 24:5463–5475

Cudmore S, Reckmann I, Way M (1997) Viral manipulations of the actin cytoskeleton. Trends Microbiol 5:142–148

Dharan NJ, Gubareva LV, Meyer JJ, Okomo-Adhiambo M, McClinton RC, Marshall SA, St George K, Epperson S, Brammer L, Klimov AI et al (2009) Infections with oseltamivir-resistant influenza A (H1N1) virus in the United States. JAMA 301:1034–1041

Galluzzi L, Vitale I, Aaronson SA, Abrams JM, Adam D, Agostinis P, Alnemri ES, Altucci L, Amelio I, Andrews DW et al (2018) Molecular mechanisms of cell death: recommendations of the Nomenclature Committee on Cell Death 2018. Cell Death Differ 25:486–541

Heo Y, Cho Y, Ju KS, Cho H, Park KH, Choi H, Yoon JK, Moon C, Kim YB (2018) Antiviral activity of *Poncirus trifoliata* seed extract against oseltamivir-resistant influenza virus. J Microbiol 56:586–592

Marjuki H, Mishin VP, Chesnokov AP, De La Cruz JA, Davis CT, Villanueva JM, Fry AM, Gubareva LV (2015a) Neuraminidase mutations conferring resistance to oseltamivir in influenza A(H7N9) viruses. J Virol 89:5419–5426

Marjuki H, Mishin VP, Chesnokov AP, Jones J, De La Cruz JA, Sleeman K, Tamura D, Nguyen HT, Wu HS, Chang FY et al (2015b) Characterization of drug-resistant influenza A(H7N9) variants isolated from an oseltamivir-treated patient in Taiwan. J Infect Dis 211:249–257

Miki H, Setou M, Kaneshiro K, Hirokawa N (2001) All kinesin superfamily protein, KIF, genes in mouse and human. Proc Natl Acad Sci USA 98:7004–7011

Radtke K, Dohner K, Sodeik B (2006) Viral interactions with the cytoskeleton: a Hitchhiker's guide to the cell. Cell Microbiol 8:387–400

Ramos-Nascimento A, Kellen B, Ferreira F, Alenquer M, Vale-Costa S, Raposo G, Delevoye C, Amorim MJ (2017) KIF13A mediates trafficking of influenza A virus ribonucleoproteins. J Cell Sci 130:4038–4050

Schnapp BJ (2003) Trafficking of signaling modules by kinesin motors. J Cell Sci 116:2125–2135

Smith AE, Helenius A (2004) How viruses enter animal cells. Science 304:237–242

Sodeik B (2000) Mechanisms of viral transport in the cytoplasm. Trends Microbiol 8:465–472

Valentine MT, Fordyce PM, Krzysiak TC, Gilbert SP, Block SM (2006) Individual dimers of the mitotic kinesin motor Eg5 step processively and support substantial loads in vitro. Nat Cell Biol 8:470–476

Waitzman JS, Rice SE (2014) Mechanism and regulation of kinesin-5, an essential motor for the mitotic spindle. Biol Cell 106:1–12

Wolfstein A, Nagel CH, Dohner K, Allan VJ, Sodeik B (2004) In vitro microtubule transport of viral capsids. Eur J Cell Biol 83:47–47